

Experimental study of the interaction between an inducer and impeller at very low flow rates

Victor Gentis, Michael Pereira, Florent Ravelet, Farid Bakir, Loic Pora, Petar

Tomov

► To cite this version:

Victor Gentis, Michael Pereira, Florent Ravelet, Farid Bakir, Loic Pora, et al.. Experimental study of the interaction between an inducer and impeller at very low flow rates. 12th Cavitation Symposium, 2024, Chania Crète, Greece. hal-04566037

HAL Id: hal-04566037 https://hal.science/hal-04566037

Submitted on 2 May 2024

HAL is a multi-disciplinary open access archive for the deposit and dissemination of scientific research documents, whether they are published or not. The documents may come from teaching and research institutions in France or abroad, or from public or private research centers. L'archive ouverte pluridisciplinaire **HAL**, est destinée au dépôt et à la diffusion de documents scientifiques de niveau recherche, publiés ou non, émanant des établissements d'enseignement et de recherche français ou étrangers, des laboratoires publics ou privés.

Experimental study of the interaction between an inducer and impeller at very low flow rates

^{*}V Gentis^{1,2}, M Pereira¹, F Ravelet¹, F Bakir¹, L Pora² and P Tomov²; ¹Arts et Metiers Institute of Technology, CNAM, LIFSE, HESAM University, 75013 Paris, France ²Safran Aircraft Engines, Safran Group, Réau, France

Abstract. This study aims to highlight the interactions between an inducer and an impeller, two key components of a centrifugal pump. Two configurations are studied: *inducer alone* and *inducer and impeller. Low flow-rates (3% \phi_n, 30% \phi_n, 60% \phi_n)* and low-pressure conditions, for which cavitation occurs, are investigated. The hydromechanical performance is studied and compared for both configurations, and cavitation formation is depicted using a high-speed camera. It has been shown that two types of cavitation occur: *tip vortex cavitation* and cavitation induced by *inlet prerotation*. Both types are dependent on inlet pressure and flow rate. The former does not significantly impact the head pressure coefficient, whereas the latter grows as the inlet pressure decreases and eventually causes the pump stall when reaching the blades. Furthermore, inlet pre-rotation is exacerbated by the presence of the impeller, deteriorating the overall pump performance. Despite the inducer's stall, the pump is still capable of pressurizing the fluid, and the impeller seems to compensate a percentage of the pressure drop by increasing its own contribution.

Keywords: centrifugal pump, inducer, impeller, interaction, cavitation, prerotation, low flow rates

1. Introduction

Low-pressure aircraft engines fuel pumps are utilized to pressurize fluid and to feed aircraft engines. They typically consist of three key components: an axial inducer, a centrifugal impeller and a volute casing. The primary purpose of the inducer is to prevent cavitation within the impeller by gradually increasing the fluid pressure, while the impeller allows a more significant pressure gradient to meet requirements by imparting kinetic energy to the fluid. Subsequently, this energy is converted into static pressure as the fluid traverses through the pump's volute casing. Under particularly extreme conditions, such as very low flow rates compared to the pump's nominal flow rate or very low-pressure conditions, the inducer may stall, leading to cavitation formation and instabilities occurrence that could result in the degradation of hydraulic performance or, in worst cases, pump failure [1,2]. In the current state of the art, inducer and impeller are designed independently. The overall pump's hydraulic performance is assessed through numerical and experimental validation. The interaction and matching between these two components is therefore not considered during the design process [3,4,5].

The current study aims to examine two pump configurations and explore the interaction of the inducer and the impeller under low-flow and low-pressure conditions. Hydraulic performance is investigated, and cavitation development is documented using a high-speed camera.

2. Experimental setup and experimental procedure

1.1. Experimental test bench

The test bench, as shown in figure 1, comprises different elements: the pump which is powered by an electrical motor; the upstream inducer, situated within a circular transparent section to facilitate high-speed camera visualization of upstream flow; an electromagnetic flowmeter, a circulating pump and a motorized valve used to regulate flowrate. Additionally, there is an upstream tank with a free surface connected to a vacuum pump, which allows for the regulation of the pressure system. Finally, pressure and temperature sensors enable continuous monitoring of the physical parameter, which are acquired through a data acquisition card.

As shown in figure 1, two different pump configurations are experimentally examined at low flow rates using water at ambient temperature as the working fluid. Cavitation is documented through the use of a high-speed camera (800x500, 1000fps) mounted on a tripod to avoid any vibrations from the

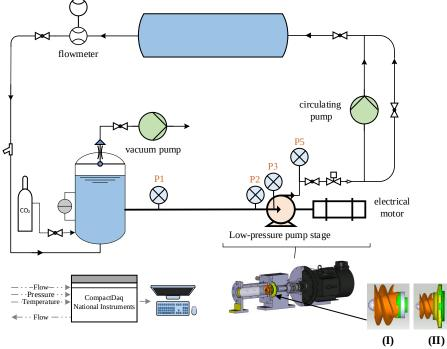


Figure 1: Test bench schematic; two configurations: Inducer alone (I) and Inducer and Impeller (II). motor.

1.2. Experimental test procedure

The cavitating test procedure can be described as follows: the pump's rotation and flow rate are initially set using a power inverter and the regulating valve. Once the pressure measurements stabilize at atmospheric pressure, the vacuum pump is turned on in order to gradually reduce the inlet static pressure. Pressure variation must be quasi-steady to minimize transitory effects. The inlet pressure is reduced until the pump fails and the pressure coefficient drops.

3. Results

1.3. Cavitation formation at low flow-rates

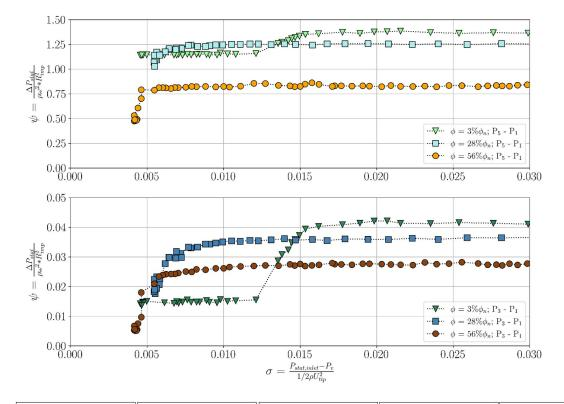
Pumps that operate at very low flow-rates are prone to cavitation formation and instability occurrence. In this section, the pump's rotation speed is $\Omega = 5000$ RPM and flow rates tested are $\phi = [3\% \phi_n; 28\% \phi_n; 56\% \phi_n]$ with ϕ , the flow coefficient defined as follow: $\phi = \frac{Q_v}{\pi \omega R_t^3}$ and ϕ_n , the pump's nominal flow

coefficient.

According to high-speed camera visualization in figure 2, the first type of cavitation observed is *tip vortex cavitation* caused by shear forces between recirculating flow and blades tip. This generates a vortex, with high vorticity and low-pressure in its core, leading to fluid vaporization [1,6,8]. Tip vortex cavitation is highly correlated to rotation speed and pressure gradient between suction and pressure sides. A higher rotation speed leads to a high-pressure gradient causing tip vortex cavitation to occur at higher inlet pressure. According to the evolution of head pressure coefficient curve in figure 2, tip vortex cavitation does not significantly impact pressure coefficient. The second type of cavitation conspicuously perceived is cavitation induced by *inlet prerotation* and backflow. Upstream flow is supposedly bereft of any vorticity. However, the inducer with high rotation speed transmits energy to the fluid, and backflow creates an annular region of negative axial velocity and nonzero

tangential velocity. For low flow rates or when reducing inlet pressure, backflow intensifies due to steep pressure gradients between downstream and upstream regions of the pump.

As illustrated in figure 2, reducing the inlet pressure, at constant flow rates, causes the inlet prerotation to expand further upstream and increases its diameter. Inlet prerotation initially occurs in the middle of the duct section attached to the hub and then reaches the periphery as it extends upstream. At σ = 0.0206, inlet prerotation occupies around half of the inlet section, supposedly altering flow incidence angles and velocities/pressure distributions, and deteriorating the hydromechanical pump performance. Eventually, when cavitation induced by pre-swirl flow has sufficiently extended radially and reaches the lower part of the blade, head pressure coefficient experiences a substantial drop causing the pump head breakdown and partly reducing the flow rate



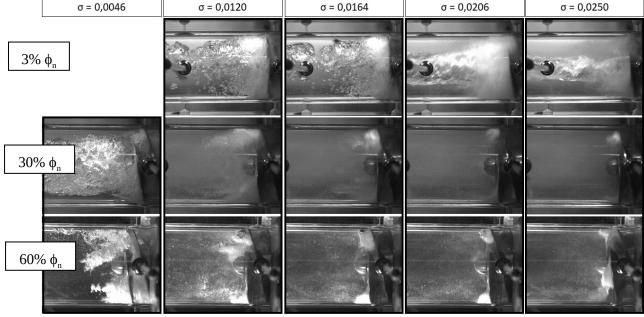


Figure 2: comparison of head pressure coefficient ψ vs cavitation number σ curves and high-speed camera visualisation for configuration (II) at Ω = 5000 RPM and ϕ = [3% ϕ_n , 30% ϕ_n , 60% ϕ_n].

1.4. Comparison of the two configurations

The primary objective of this study is to examine the interaction between the inducer and the impeller. Therefore, the two configurations are compared. The rotation speed and flow rate are respectively set at $\Omega = 6800$ RPM and $\phi = 3\% \phi_n$. Figure 3 displays the hydromechanical performance of the two configurations compared with flow visualization. The white hexagonal curve depicts the evolution of the head pressure coefficient for the *inducer alone (I)* as the inlet pressure is decreased, while the purple curve shows inducer's head pressure coefficient in the *inducer and impeller (II)* configuration.

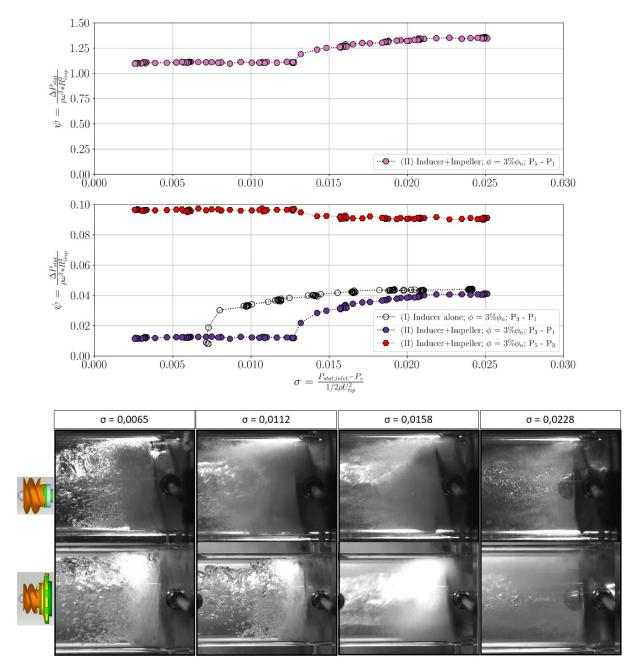


Figure 2: comparison of configuration (I) and (II) at Ω = 6800 RPM and ϕ = 3% ϕ_n .

Based on this plot, one can state that the inducer does not display the same performance whether is operates with or without the centrifugal impeller. While the head pressure coefficient is higher at atmospheric pressure in configuration (II), it experiences a pressure drop at a higher inlet NPSH value than in configuration (I). The inducer alone operates over a wider range of NPSH values, illustrating good performance even when cavitation occurs. When comparing the trends of the curves and the high-speed camera visualization, one can observe that the inlet prerotation is largely developed when

the head pressure coefficient starts to slowly decrease around $\sigma = 0.0158$, for both configurations. At $\sigma = 0.0112$, the inducer continues to pressurize the fluid in configuration (I), while it appears almost completely ineffective in the other configuration, even though it can be noted that the inducer's head pressure coefficient is not equal to zero. This could suggest that, despite the formation of cavitation within the inducer, it is still able to slightly pressurize and guide the fluid, preventing the entire system from failing. This is supported by the pink curve, which depicts overall pump performance. After experiencing the inducer pressure drop, at the same cavitation number, the stage pump continues to significantly pressurize the fluid and maintaining flow rate within the pump. Not only is the pump still able to pressure decline by increasing its own contribution depicted in the red hexagonal curve. Finally, at σ =0.0112, one can observe the inducer's head breakdown in configuration (I).

On the vertical slope of the head pressure coefficient curves, one can observe instabilities causing pressure and flow fluctuations [1,7,9]. This results in the periodic fluctuation in size and intensity of the inlet prerotation cavitation phenomenon. Once the inlet backflow-induced reaches the blades, it will be transported within the inducer and collapse, allowing the flow to penetrate more easily inside the pump. The cavitation then develops again, and the cycle repeats. The frequency of cavitation formation, that can be determined using high-speed camera, also fluctuates, and eventually, the inducer fails, reducing the pressure gradients between the suction and pressure sides, thus preventing backflow and inlet prerotation cavitation for occurring. Flow visualization at inlet pressure lower than critical NPSH value shows that inlet prerotation is no longer developing upstream the inducer. In fact, one can suppose that inducer no longer transmits energy to the fluid anymore, but instead, water flows through tip clearance driven by the impeller and guided by the inducer.

4. Conclusion

Two configurations – inducer alone and inducer mounted with the impeller - have been experimentally studied at low flow rates (3% ϕ_n , 30% ϕ_n , 60% ϕ_n). Cavitation occurs at higher inlet pressure at low flow rate, causing head pressure coefficient to start decreasing at NPSH values close to the value of the atmospheric pressure. On the other hand, at higher flow rates, head pressure remains steady for most of the cavitation number range. At some point, backflow inlet prerotation develops extremely fast and causes a steep drop of head pressure coefficient curve. On the vertical slope of the head curve, pump is prone to experiencing instabilities, causing flow rate and pressure fluctuations. The frequency of theses instabilities shifts as we continue to reduce the cavitation number, and eventually, the cavitation collapses, leading to inducer stall. Even though the inducer does not efficiently pressurize the fluid, the pump is still able to operate, and the centrifugal impeller still entrain the fluid, struggling to maintain the flow rate.

These observations highlight the interactions between the inducer and the impeller and raise questions about the design process, particularly the impeller pressure requirements. In future work, two additional configurations will be tested: impeller alone and inducer and impeller with an axial gap. The former will allow us to characterize inlet pressure requirements while the latter will provide a better understanding of the interaction between these two components. Frequency of inlet prerotation and other types of cavitation will be investigated using dynamic pressure sensors for all configurations.

5. Acknowledgement

The authors would like to acknowledge the financial support granted by SAFRAN Aircraft Engines for the PhD thesis.

6. References

- [1] Brennen CE. 2011 Mar 28 Hydrodynamics of pumps. Cambridge University Press.
- [2] Brennen CE. 2014 Cavitation and bubble dynamics. Cambridge University Press.
- [3] Wang D, Gao B, Chen Y, Pan Y, Luo J, Liu L, Wei Q, Liu L. 2023 Jan 20 Effects of Matching between the Inducer and the Impeller of a Centrifugal Pump on Its Cavitation Performance. Machines. 11(2):142.
- [4] Yang B, Li B, Chen H, Liu Z, Xu K. 2019 Jul 1 Numerical investigation of the clocking effect between inducer and impeller on pressure pulsations in a liquid rocket engine oxygen turbopump. Journal of Fluids Engineering. 141(7):071109.
- [5] Bakir F, Kouidri S, Noguera R, Rey R. 1998 Jun 21 Design and analysis of axial inducers performances. In ASME Fluids Engineering Division Summer Meeting. Washington DC, USA (Vol. 60).
- [6] Ito Y, Tsunoda A, Kurishita Y, Kitano S, Nagasaki T. 2016 Jan Experimental visualization of cryogenic backflow vortex cavitation with thermodynamic effects. Journal of Propulsion and Power. 32(1):71-82.
- [7] Bhattacharyya A, Acosta AJ, Brennen CE, Caughey TK. 1993 Observations on Off-Design Flows in Non-Cavitating Axial Flow Inducers. In ASME Symposium on Pumping Machinery (No. 154, pp. 135-141). American Society of Mechnical Engineers.
- [8] Magne T, Paridaens R, Khelladi S, Bakir F, Tomov P, Pora L. 2020 Nov 1 Experimental Study of the Hydraulic Performances of Two Three-Bladed Inducers in Water, Water With Dissolved CO2, and Jet Fuel. Journal of Fluids Engineering. 142(11):111210.
- [9] Yamamoto K, Tsujimoto Y. 2009 A backflow vortex cavitation and its effects on cavitation instabilities. International Journal of Fluid Machinery and Systems. 2(1):40-54.